Ultrasonics Sonochemistry 23 (2015) 37–45

Contents lists available at ScienceDirect

Ultrasonics Sonochemistry

journal homepage: www.elsevier.com/locate/ultson

New interpretation of the effects of argon-saturating gas toward sonochemical reactions

Slimane Merouani [a,b,*], Hamza Ferkous [a], Oualid Hamdaoui [a], Yacine Rezgui [c], Miloud Guemini [c]

[a] Laboratory of Environmental Engineering, Department of Process Engineering, Faculty of Engineering, Badji Mokhtar – Annaba University, P.O. Box 12, 23000 Annaba, Algeria
[b] Department of Chemical Engineering, Faculty of Pharmaceutical Engineering Process, University of Constantine 3, 25000 Constantine, Algeria
[c] Laboratory of Applied Chemistry and Materials Technology, University of Oum El-Bouaghi, P.O. Box 358, 04000 Oum El Bouaghi, Algeria

ARTICLE INFO

Article history:
Received 30 July 2014
Received in revised form 12 September 2014
Accepted 18 September 2014
Available online 28 September 2014

Keywords:
Sonochemical activity
Saturating gases
Single bubble
Computer simulations
·OH radical

ABSTRACT

A number of literature reports showed that argon provides a more sonochemical activity than polyatomic gases because of its higher polytropic ratio; whereas several recent studies showed that polyatomic gases, such as O_2, can compensate the lower bubble temperature by the self decomposition in the bubble. In this work, we show for the first time a numerical interpretation of these controversial reported effects. Computer simulations of chemical reactions inside a collapsing acoustic bubble in water saturated by different gases (Ar, O_2, air and N_2) have been performed for different frequencies (213–1100 kHz). In all cases, ·OH radical is the main powerful oxidant created in the bubble. Unexpectedly, the order of saturating gases toward the production rate of ·OH radical was strongly frequency dependent. The rate of production decreases in the order of Ar > O_2 > air > N_2 for frequencies above 515 kHz, and Ar starts to lose progressively its first order to the following gases with a gradually decreasing of frequency below 515 kHz up to a final order of O_2 > air ~ N_2 > Ar at 213 kHz. The analysis of chemical kinetic results showed a surprising aspect: in some cases, there exists an optimum bubble temperature during collapse at which the chemical yield is much higher than that of the maximum bubble temperature achieved in the bubble. On the basis of this, we have concluded that the lower sonochemical activity induced by Ar for frequencies below 515 kHz is mainly due to the forte consumption of radicals inside a bubble prior the complete collapse being reached.

1. Introduction

When a liquid containing dissolved gas is irradiated by an ultrasound wave, many tiny bubbles appear which is a phenomenon known as acoustic cavitation [1]. The bubbles repeat expansion and contraction according to the pressure oscillation of an ultrasonic wave [1]. Some bubbles collapse violently at the contraction phase and extreme temperature and pressures are developed therein (several thousands of Kelvin and several hundreds of atmospheres) [2]. Under such conditions molecules trapped in the bubble (water vapor, gases and vaporized solutes) can be brought to an excited-state and dissociate. As results, reactive species such as ·OH, HO_2, H·, O and H_2O_2 are created from H_2O and O_2 dissociation and their associate reactions in the bubble [3]. These chemical products may diffuse out of the bubble and dissolve in the surrounding liquid [4]. Reactions involving free radicals can occur within the collapsing bubble, at the liquid interface and in the surrounding liquid [4]. Solutes, i.e. aqueous pollutants, can easily oxidized by the oxidants such as ·OH, which is considered the primary oxidizing species during aqueous sonolysis. The chemistry using acoustic cavitation is called sonochemistry. Sonochemistry is one of the recent advanced oxidation processes for water and wastewater treatment. Cavitation bubbles due to the very high temperatures generated at the final stages of bubble collapse emit light, which is known as sonoluminescence [5].

The sonochemical activity (production of radicals) is influenced by a number of factors such as frequency of ultrasound, dissolved gas, acoustic power and liquid temperature [6–12]. Among these factors, the nature of the dissolved gases have shown controversial effects, particularly differences between argon and polyatomic gases. A number of experimental reports [13–16] showed that argon provides a more sonochemical activity than polyatomic gases because of its higher polytropic ratio, which yields higher bubble temperature at the collapse. Whereas several other studies [9,11,12,17–20] showed that polyatomic gases, such as O_2, can compensate the lower O_2-bubble temperature by the self-decomposition in the bubble and then yield more sonochemical

* Corresponding author. Tel./fax: +213 (0)38876560.
E-mail address: s.merouani@yahoo.fr (S. Merouani).

http://dx.doi.org/10.1016/j.ultsonch.2014.09.009
1350-4177/

Nomenclature

c	speed of sound in the liquid medium, (m s^{-1})
f	frequency of ultrasonic wave, (Hz)
I_a	acoustic intensity of ultrasonic irradiation, (W m^{-2})
p	pressure inside a bubble, (Pa)
p_{max}	maximum pressure inside a bubble (Pa)
p_∞	ambient static pressure, (Pa)
P_A	amplitude of the acoustic pressure, (Pa)
P_v	vapor pressure of water, (Pa)
P_{g0}	initial gas pressure, (Pa)
R	radius of the bubble, (m)
R_{max}	maximum radius of the bubble, (m)
R_0	ambient bubble radius, (m)
t	time, (s)
T	temperature inside a bubble, (K)
T_{max}	maximum temperature inside a bubble, (K)
T_{opt}	optimum bubble temperature for the production of ·OH radical, (K)
T_∞	bulk liquid temperature, (K)
x_i	solubility (in mole fraction) of the gas i in water

Greek letters

γ	specific heat ratio (c_p/c_v) of the mixture
σ	surface tension of liquid water, (N m^{-1}).
ρ	density of liquid water, (kg m^{-3}).
λ	gas thermal conductivity, (W m^{-2} K).

activity than argon. Therefore, the mechanism of the argon-induced lower or higher sonochemical activity than polyatomic gases is until now not understood. The present work deals with studying the effects of some saturating gases in scale of single-bubble for a possible explanation of these controversial results reported in the literature. Computer simulations of chemical reactions occurring inside a collapsing acoustic bubble in water saturated by different gases (Ar, O_2, air and N_2) have been performed for different frequencies (213–1100 kHz). The employed model combines the dynamic of bubble collapse in acoustic field with the chemical kinetics occurring in the bubble during the strong collapse.

2. Model and computational methods

The theoretical model used in the present numerical simulations has been described in our previous works [21,22]. The following is a brief description of the model.

2.1. Bubble dynamics model

A gas and vapor filled spherical bubble isolated in water oscillates under the action of a sinusoidal sound wave. The temperature and pressure in the bubble are assumed spatially uniform and the gas content of the bubble behaves as an ideal gas [23]. The radial dynamics of the bubble is described by the Keller equation that includes first order terms in the Mach number $\dot{R}/c$ [24,25]:

$$\left(1-\frac{\dot{R}}{c}\right)R\ddot{R}+\frac{3}{2}\left(1-\frac{\dot{R}}{3c}\right)\dot{R}^2 = \frac{1}{\rho_L}\left(1+\frac{\dot{R}}{c}+\frac{R}{c}\frac{d}{dt}\right)\left[p-p_\infty-\frac{2\sigma}{R}-4\mu\frac{\dot{R}}{R}+P_A\sin(2\pi ft)\right] \quad (1)$$

in this equation dots denote time derivatives (d/dt), R is the radius of the bubble, c is the speed of sound in the liquid, ρ_L is the density of the liquid, σ is the surface tension, μ is the liquid viscosity, p is the pressure inside the bubble, p_∞ is the ambient static pressure, P_A is the acoustic amplitude and f is the sound frequency. The acoustic amplitude P_A is correlated with the acoustic intensity I_a, or power per unit area, as $P_A = (2I_a\rho_L c)^{1/2}$ [4].

The expansion of the bubble is assumed as isothermal and its total compression is considered as adiabatic [26]. These assumptions, which are widely accepted since the lifetime of an oscillation at high frequency is relatively short with a very rapidly occurring collapse event, were pointed out by Yasui et al. [27] using a more detailed model. We also assume that the vapor pressure in the bubble remains constant during the bubble expansion phase and there is no gas diffusion during expansion and no mass and heat transfer of any kind during collapse. We note here that Storey and Szeri [28] demonstrated that the inclusion of mass transfer (non-equilibrium condensation and evaporation and gas diffusion at the bubble wall) on the bubble dynamics has practically no effect on the maximum bubble temperature attained in the bubble at the collapse when the compression ratio of the bubble (R_{max}/R_{min}) is less than 20 (R_{max} is the maximum radius of the bubble and R_{min} is the minimum bubble radius at the collapse). This level of R_{max}/R_{min} was never attained in the present numerical study. Therefore, in order to reduce computational parameters, the current model takes, as input, initial bubble vapor content and neglects mass and heat transfer during bubble expansion and collapse.

Based on the above assumptions, the pressure and temperature inside the bubble at any instant during the collapse phase can be calculated from the bubble size as

$$p = \left[P_v + P_{g0}\left(\frac{R_0}{R_{max}}\right)^3\right]\left(\frac{R_{max}}{R}\right)^{3\gamma} \quad (2)$$

$$T = T_\infty\left(\frac{R_{max}}{R}\right)^{3(\gamma-1)} \quad (3)$$

where P_v is the vapor pressure, $P_{g0} = p_\infty + (2\sigma/R_0) - P_v$ is the gas pressure in the bubble at its ambient state ($R = R_0$), R_0 is the ambient bubble radius, T_∞ is the bulk liquid temperature and γ is the ratio of specific heats capacities (c_p/c_v) of the gas/vapor mixture. The maximum internal temperature (T_{max}) and pressure (p_{max}) in the bubble are reached at the end of the bubble collapse and they are approximated by:

$$T_{max} = T_\infty\left(\frac{R_{max}}{R_{min}}\right)^{3(\gamma-1)} \quad (4)$$

$$p_{max} = \left[P_v + P_{g0}\left(\frac{R_0}{R_{max}}\right)^3\right]\left(\frac{R_{max}}{R_{min}}\right)^{3\gamma} \quad (5)$$

It is important to notice here that the assumption of spatial uniform pressure and temperature inside the bubble is valid as long as inertia effects are negligible and the velocity of the bubble wall is below the speed of sound in the vapor/gas mixture. This assumption was justified in detail in the paper published by Kamath et al. [29]. In addition, several researchers [27,30–32] pointed out in their models which include heat transfer that the bubble temperature and pressure are roughly uniform except at a very thin layer, called thermal boundary, near the bubble wall.

2.2. Chemical kinetics model

For Ar and O_2 bubbles, a kinetic mechanism consisting in 25 chemical reactions and their backwards reactions (the first 25 reactions of Table 2 in Ref. [22]) [21,26,29] is taken into account involving O_2, H_2O, $^{\cdot}OH$, $H^{\cdot}$, O, $HO_2^{\cdot}$, O_3, H_2 and H_2O_2 species. For air and N_2 bubbles, a kinetic mechanism consisting in 73 chemical reactions and their backwards reactions (all reactions of Table 2 in Ref. [22]) [33–35] is taken into account including, in addition to those involved in an O_2 bubble, N_2, N, NO, NO_2, NO_3, HNO_2, HNO_3, N_2O, HNO, NH, NH_2, NH_3, N_2H_2, N_2H_3, N_2H_4, N_2O_4 and N_2O_5 species. Detailed information about the kinetic mechanisms used in the present numerical calculations is available in our previous paper [22].

The chemical kinetics model consists of the reaction mechanism and determines the production of each species during the bubble collapse. The detail of the chemical kinetics model used for the simulation of the reactions systems have been described elsewhere [36].

2.3. Procedure of the numerical simulation

The numerical procedure used for solving the bubble dynamic equation and simulating the reactions systems inside a bubble have been presented in detail in our previous work [36]. It should be noticed here that although the chemical reactions occurring in the cavity were classified as endothermic and can cool the bubble at higher temperature than 10,000 K [37], their effects on the bubble dynamics is known to be not significant when the bubble temperature is much lower than 10,000 K [28,38]. This temperature, 10,000 K, was never attained in our numerical simulations. The dynamics output results, thus, will not greatly affected by the chemical reactions. This effect is not taken into account in the present numerical investigation.

3. Results and discussion

In the present work, numerical simulations of chemical reactions occurring inside Ar, O_2, air and N_2 bubbles have been performed for different ultrasonic frequencies in the range of 213–1100 kHz when the acoustic intensity and the bulk liquid temperature were 1 W cm^{-2} and 20 °C, respectively. On the other hand, it is known that the ambient radius (R_0) for a typical active bubble depends on the experimentally controllable parameters, principally to the driving ultrasonic frequency [39–42]. The present study tries to use the same frequencies at which the mean ambient bubble radii (R_0) were determined experimentally. The ambient bubble radius (R_0) in the present numerical simulations has been assumed as the mean ambient bubble radius. The selected values of R_0 and frequency are presented in Table 1. In general, the nature of the dissolved gases does not affect significantly the initial size of the bubble. This is confirmed using numerical simulation for various R_0 and different saturating gases (Ar, air and O_2) where we found that the range and the optimum value of R_0, which represent the mean initial size of active bubble, are exactly the same for the different gases (data not shown).

Table 1
Selected values of the ambient bubble radius (R_0) for active bubbles as function of frequency of ultrasound.

Frequency (kHz)	Ambient bubble radius, R_0 (μm)	References
213	3.9	[39]
355	3.2	[39]
515	3	[43]
647	2.9	[39]
875	2.7	[39]
1100	1.4	[44]

3.1. Bubble dynamics and chemical bubble yield

A series of numerical simulations of the bubble oscillation have been performed for different conditions of saturating gas and frequency. In all cases, it was found that the bubble expands during the rarefaction part of ultrasound wave until a maximum size being reached and then violently collapses to a minimum size during the compression part of ultrasound wave. Fig. 1 shows the variation of the calculated bubble radius and temperature inside a bubble as function of time during the collapse of a bubble driven by an ultrasound frequency of 355 kHz under argon and oxygen saturating atmospheres. It was seen that the bubble compresses very violently up to 3% of its maximum radius in the case of O_2-bubble (5% in the case of Ar-bubble) and then goes to an equilibrium state before a successive expansion phase. The temperature inside a bubble starts with a slow increase during the first stage of the collapse and then increases suddenly at the end of the bubble collapse up to 3550 and 5300 K for O_2 and Ar bubbles, respectively. The same behavior has been observed for the internal bubble pressure that attained 578 and 125 atm for respectively O_2 and Ar bubbles. Fig. 1 also showed that although the minimum bubble size reached for Ar saturated liquid is larger than O_2 saturated liquid, the temperature for Ar is higher. This is due to the higher polytropic ratio of argon, $\gamma_{Ar} = 1.66$, compared to that of O_2, $\gamma_{O2} = 1.41$ (the bubble temperature depends on both the polytropic ratio and the compression ratio R_{max}/R_{min} as shown in

Table 2
Dependence of the order of the saturating gases effect on the driving ultrasonic frequency in some literature experimental sonochemical phenomenons.

Work	Description	Frequency (kHz)	Order
Nagata et al. [50]	Sonochemical decomposition of hydroxybenzoic acids in water	200	Air > Ar
Torres et al. [9]	Production of H_2O_2 and oxidation of bisphenol A in water	300	O_2 > Air > Ar
Arriage et al. [52]	Production of H_2O_2 and oxidation of ibuprofen in water	300	O_2 > Air > Ar
Hart and Henglein [51]	Production of H_2O_2 in water	300	O_2 > H_2
Mark et al. [20]	Fricke dosimetry	321	O_2 > Air > Ar
Beckett and Hua [11]	1,4-Dioxane oxidation and sonoluminescence intensity	358	O_2 > Ar
Mead et al. [12]	Production of H_2O_2 in water	447	O_2 > Air > Ar > N_2
Hua et Hoffman [13]	Production of H_2O_2 in water	513	Ar > O_2
–	Production of H_2O_2 in water*	575	Ar > Air > N_2
Gao et al. [16]	Oxidation of sulfa-methazine in water	800	Ar > O_2 > Air > N_2
Guzman-Duque et al. [15]	Oxidation of crystal violet in water	800	Ar > Air
–	Production of H_2O_2 in water*	875	Ar > Air > N_2
		1140	

* Experiments carried out in our laboratory. The employed reactor (generator/transducer/cell arrangement) and methods for quantifying H_2O_2 were described in our previous work [36].

Eq. (3)). It should be noted that for air and N_2 bubbles, the results are the same as those of O_2 bubble as all these polyatomic gases have the same polytropic ratio (γ = 1.41), which differs from that of Ar (γ_{Ar} = 1.66).

In Fig. 2(a)–(d), the calculated results of the chemical reactions inside a bubble are shown as function of time at around the end of the bubble collapse for various saturating gases. Under the very high temperatures developed in the bubble at the last stage of the collapse, chemical reactions occur in time scale of several nanoseconds and many chemical products such as ·OH, $HO_2^{\cdot}$, H·, O, H_2O_2 and others are formed from the dissociation of the trapped water vapor and gases and their associate reactions in the bubble. In the case of an air bubble, there is a formation of little amounts of HNO_2 and HNO_3. These two species have been detected and quantified in several experimental studies when a similar trend of higher yields of HNO_2 than HNO_3 was observed [12,45,46]. While HNO_2 is found in N_2 bubble, HNO_3 is not detected (Fig 2(d)). The dissociation of N_2 is mainly by $N_2 + O \rightarrow NO + N$ and the creation of HNO_2 is mainly by $\cdot OH + NO + M \rightarrow HNO_2 + M$. HNO_3 is formed mainly through $OH + NO_2 + M \rightarrow HNO_3 + M$. Also, several oxidizing nitrogen (NO, NO_3 and N_2O) are detected in air and N_2 bubbles. NO, which showed the higher yield among these species, is the main species responsible for the lower sonochemical activity in air and N_2 bubbles compared with O_2 bubble [47]. It was also observed that all species containing nitrogen are formed only at higher bubble temperatures, nearly at the end of the bubble collapse, whereas oxygenic products, particularly ·OH radical, started to form at low bubble temperatures. Hydroxyl radical has been specifically identified in sonicated aqueous solution via electron spin resonance [48]. The ·OH radical is considered the primary oxidizing species during aqueous sonolysis because of its high potential of oxidation than the other oxidants formed in the bubble. From Fig. 2(a)–(d), it was clearly noticed that ·OH radical is the main powerful oxidant formed in the bubble.

Another important statement that can be observed from Fig. 2(a) is the existence of an optimum temperature (~4200 K) inside an Ar-bubble that maximizes the production of some products, specifically ·OH radical. For all other gases, the production rates of ·OH radical attained their upper limit at the end of the bubble collapse at which the maximum bubble temperature is attained.

From Figs. 1 and 2, it was observed that the bubble temperature suddenly drops to the ambient temperature just after the minimum bubble radius. This behavior, which results from the assumption of the adiabatic collapse and isothermal expansion, differs slightly from that of a real situation as can be seen in Ref. [27]. However, this will not affect the calculated chemical bubble yield at the end of the bubble collapse (at R_{min}), for which are based the calculations of Fig. 3. Recently, Yasui et al. [42] developed a bubble dynamics model that includes the mass transfer and the thermal conduction phenomena and used them to predict the range of ambient radius for the production of oxidants in an air bubble. In Ref. [49], we carried out a comparison between our model and Yasui's model [42] in term of the range of ambient radius for the production of the oxidants. At 1000 kHz, Yasui et al. [42] reported a range of 0.1–3 μm. For the same conditions, we have calculated a range of ~0.3–3.8 μm with our model that neglects mass and heat transfer. The conclusion was that our results agree with the results of Yasui et al. [42] and the slightly observed difference is due to the different nature of bubbles: sonoluminescing (SL) bubble in Yasui's paper and sonochemically active bubble in our work (the range of ambient radius for SL bubble is smaller than that of sonochemically active bubble [42]). This simple comparison showed that the range of ambient bubble radius for

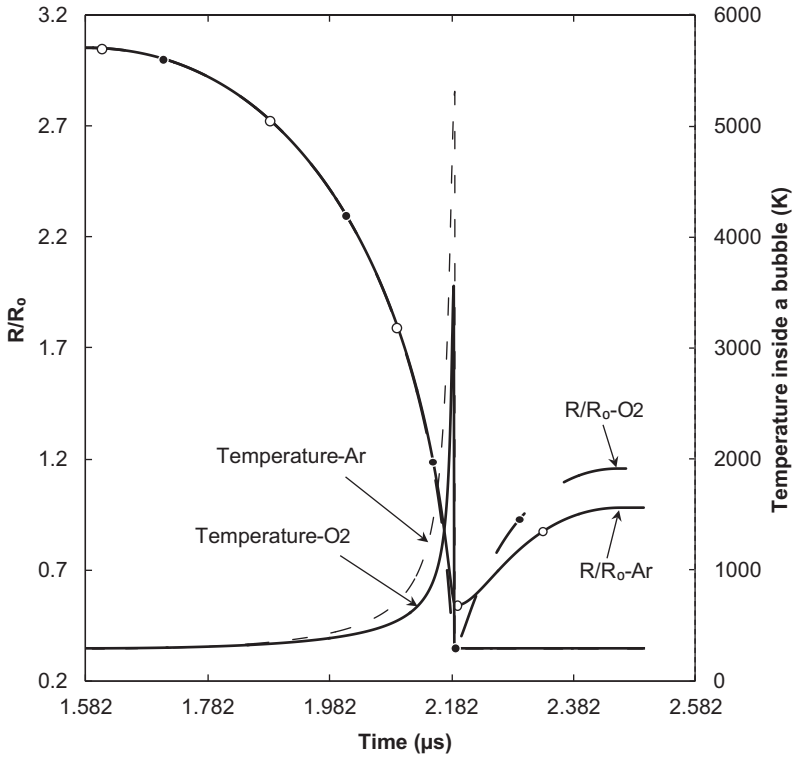

Fig. 1. Bubble radius and internal bubble temperature versus time curves during the collapse phase of the bubble for various dissolved gases (conditions: ambient bubble radius: 3.2 μm; frequency: 355 kHz; acoustic intensity: 1 W cm^{-2}; bulk liquid temperature: 20 °C; static pressure: 1 atm). The physical properties used for numerical calculations are given for water at 20 °C as ρ_L = 998.12 kg m^{-3}, σ = 72.45 × 10^{-3} N m^{-1}, μ = 10^{-3} kg s^{-1} m^{-1} and c = 1482 m s^{-1}.

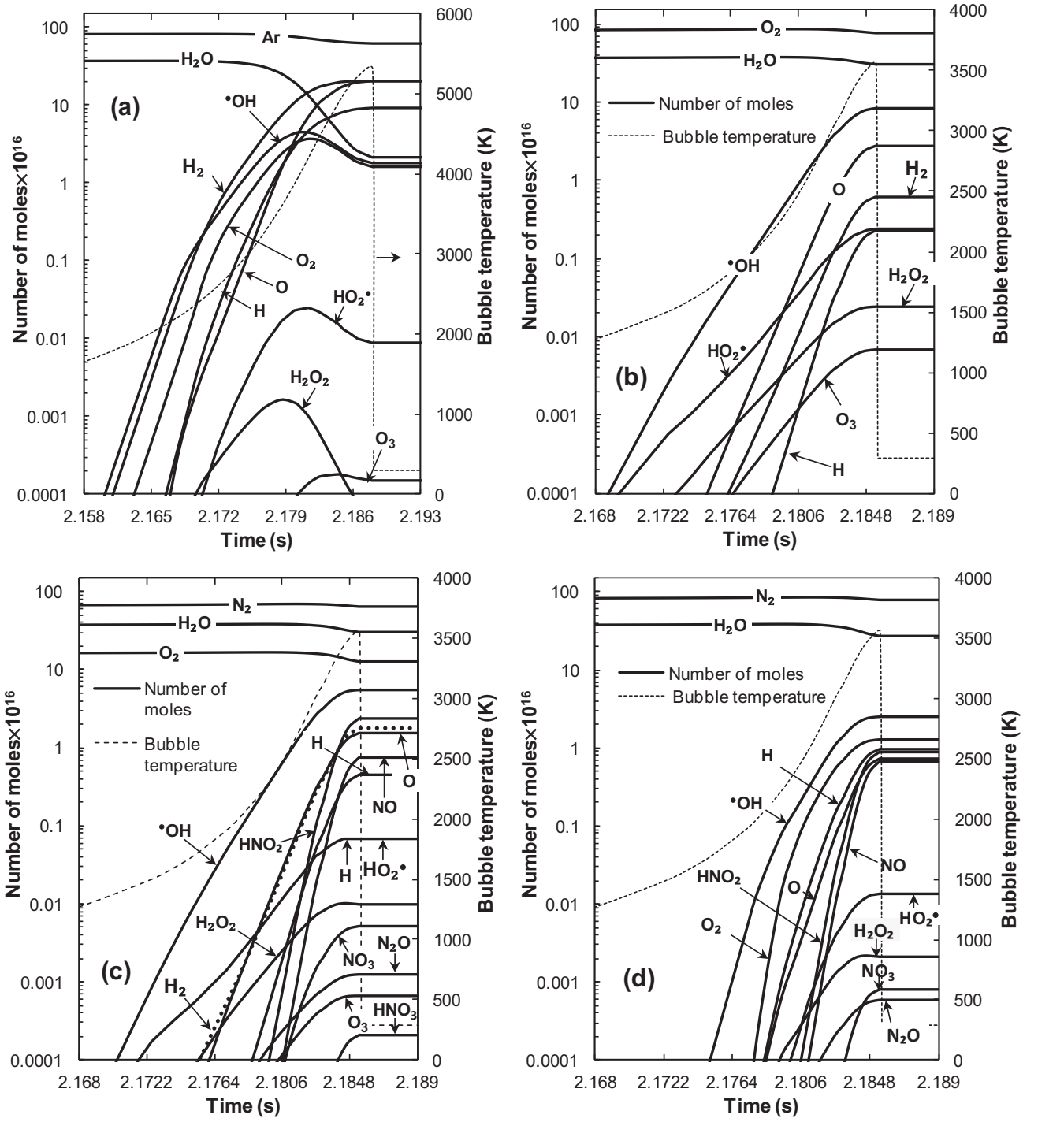

Fig. 2. Evolution of the reaction systems inside a bubble as function of time at around the end of the bubble collapse for various saturating gases, for the same conditions as in Fig. 1. (a) Ar-bubble, (b) O_2-bubble, (c) air-bubble and (d) N_2-bubble. Principal vertical axes (number of moles) are in logarithmic scale. Horizontal axes are presented for only ~0.03 μs.

the production of the oxidants is the same with and without heat and mass transfer at the bubble wall.

3.2. ·OH-production rate dependence of the nature of dissolved gases

Fig. 3 shows the effects of Ar, O_2, air and N_2 saturating gases on the production rate of ·OH radical in the bubble for various ultrasonic frequencies. The production rate of ·OH is defined as the amount of this species at the end of the first bubble collapse multiplied by the ultrasonic frequency [42]. From Fig. 3, it clearly appears that the effect of saturating gases on the production rate of ·OH radical is frequency dependent. Excluding Ar, the order follows O_2 > air > N_2 > H_2. Including Ar, the order is strongly sensitive to the ultrasonic frequency. It follows the order Ar > O_2 > air > N_2 > H_2 for frequencies above 515 kHz and then Ar starts to lose progressively its first order to the following gases with a gradually decreasing of frequency below 515 kHz up to a final order of O_2 > air ~N_2 ~ H_2 > Ar at 213 kHz. It was also

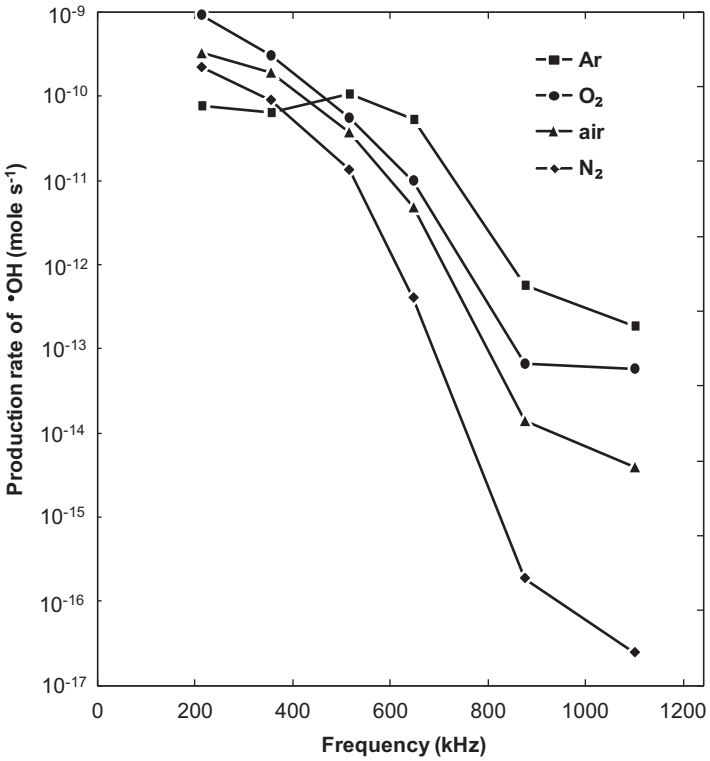

Fig. 3. Production rate of ·OH radical inside a bubble as function of ultrasonic frequency for various saturating gases (conditions: ambient bubble radius: Table 1; acoustic intensity:1 W cm^{-2}; bulk liquid temperature: 20 °C; static pressure: 1 atm). The vertical axis is in logarithmic scale. The production rate of ·OH is defined as the amount of this species at the end of the first bubble collapse multiplied by the ultrasonic frequency [42].

observed that in the case of Ar-bubble there exists an optimum frequency of about 515 kHz for the production of ·OH radical.

The effect of saturating gases toward aqueous sonochemical reactions is largely reported in the literature. However, the obtained orders observed in Fig. 3 for single bubble sonochemistry are in very good agreement with the large amount of experimental reports as can be seen in Table 2 that summarizes some of the literature experimental results.

In general, dissolved gases influence single bubble sonochemistry through three aspects [53]. Firstly, monatomic gases typically have greater polytropic indexes γ ($\gamma = c_p/c_v$) than polyatomic gases, and the higher polytropic index can result in higher temperature achieved in the bubble at the collapse. Secondly, some polyatomic gases, such as O_2, can provide a secondary source for radicals' production by the self pyrolytic dissociation and its associate reactions inside a bubble and, thus, compensate the lower bubble temperature generated by the polyatomic gases. Thirdly, gases with low thermal conductivities (λ) can reduce the heat dissipation, thus facilitating the increase in collapse temperature (T_{max}) and enhancing sonochemical activity.

In this manuscript, argon has the greater polytropic ratio ($\gamma_{Ar} = 1.66$) and the lower thermal conductivity ($\lambda_{Ar} = 0.018$ W m^{-2} K^{-1} [54]) than O_2, air and N_2 gases that have the same γ and λ ($\gamma = 1.41$, $\lambda = 0.026$ W m^{-2} K^{-1} [54]). Therefore, the bubble implosion in the presence of Ar favors a higher bubble temperature, which is what we obtained numerically as shown in Fig. 4. It should be noted that the effect of thermal conductivity is not considered in our model as the heat transfer during bubble oscillation is ignored. However, it is important to mention that Okitsu et al. [55] showed experimentally that the bubble temperature is not affected by the gas conductivity at high ultrasound frequency. Therefore, it is not surprising that argon achieved the highest production rates of ·OH radical at high frequencies above 515 kHz. The unexpected effect is the lower production rate of ·OH radical at frequencies below 515 kHz for an argon bubble despite the higher temperatures. This trend could not be attributed to the neglected thermal conductivity because the maximum temperatures for 213 and 355 kHz are much higher than those attained at frequencies above 515 kHz (see Fig. 4). Additionally, the maximum temperatures achieved in the bubbles follow the logical order: the gas with a lower conductivity generates the highest temperature. Consequently, the logical question to be asked is why Ar provided a lower sonochemical activity than polyatomic gases for only frequencies below 515 kHz. Several authors [9,11,12,20,52] interpreted this trend by the fact that O_2 (or air) sonolysis engenders additional reactions within the gaseous bubble, which leads to the production of additional radical species during decomposition of O_2 and this can compensate the lower O_2-bubble temperature. However, if this is the case, why polyatomic gases showed lower sonochemical activity than argon for all frequencies above 515 kHz which is the phenomenon observed experimentally as well as numerically. On the other hand, the numerical simulations showed that similar products are found in Ar and O_2 bubbles (see Fig. 2(a)–(b)), which indicates that similar reactions are occurred in both Ar and O_2 bubbles. Therefore, in reality, the presence of O_2 within the bubble only accelerates or decelerates the rates of reactions involved therein and does not provide additional sources for the production of radicals in the gaseous phase. Consequently, the hypothesis of the O_2-yielded additional reactions in the bubble which compensate the lower bubble temperature is not well justified.

For a possible explanation of the unexpected effect of Ar, we have analyzed the results of the chemical kinetics as function of time during collapse for all conditions of saturating gases and frequency. Surprisingly, the analysis showed that in some cases there is an optimum bubble temperature during collapse at which the

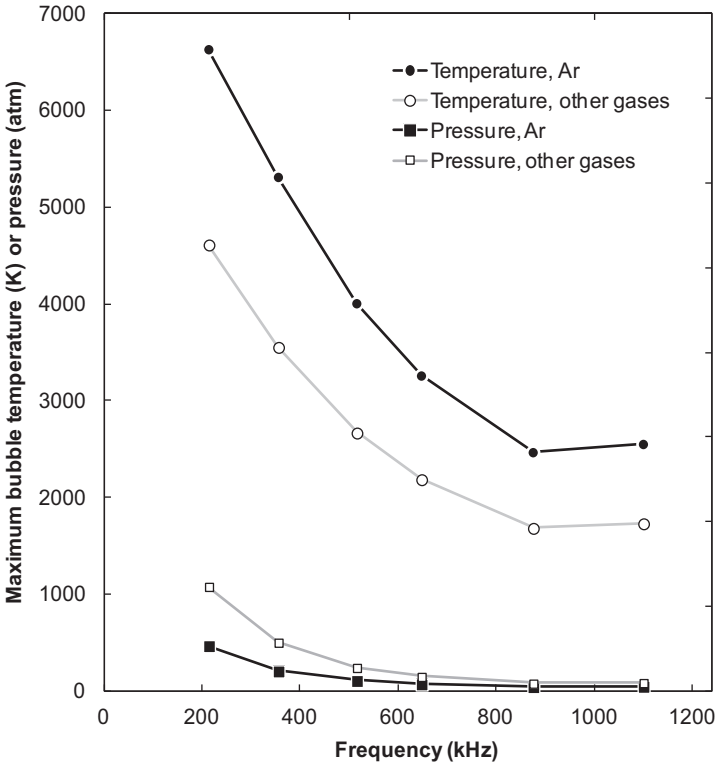

Fig. 4. Maximum bubble temperature and pressure achieved in the bubble at the end of the collapse as function of ultrasonic frequency for various dissolved gases (conditions: ambient bubble radius: Table 1; acoustic intensity: 1 W cm^{-2}; bulk liquid temperature: 20 °C; static pressure: 1 atm).

yield of ·OH is much higher than that of the maximum bubble temperature achieved in the bubble. This surprising aspect was observed only for Ar bubbles at frequencies below 515 kHz. For all other gases, the production rates of ·OH radical attained their upper limit at the end of the bubble collapse when the maximum bubble temperature is achieved. In Fig 5, the evolutions of the mole fraction of ·OH created inside an Ar-bubble as function of bubble temperature is shown for various frequencies. At 647 kHz, the

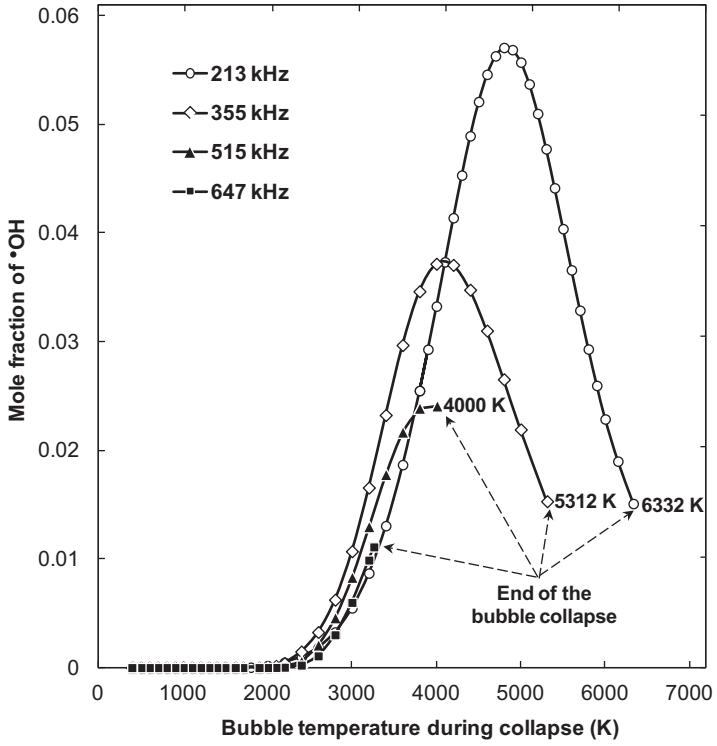

Fig. 5. Evolution of the mole fraction of ·OH radical inside an Ar-bubble as function of temperature during the collapse phase for different ultrasonic frequencies (conditions: ambient bubble radius: Table 1; acoustic intensity: 1 W cm^2; bulk liquid temperature: 20 °C; static pressure: 1 atm).

maximum production of ·OH is achieved at the end of the bubble collapse when the bubble temperature attained the maximum value (T_{max} = 3260 K). At 515 kHz, an optimum bubble temperature for the production of ·OH begins to appear at around the end of the bubble collapse ($T_{opt} \approx T_{max} \approx 4000$ K) and the production rate at this point is 2.5 times higher than that obtained at 647 kHz. At 355 kHz, an optimum bubble temperature of ~4200 K is observed, which is significantly lower than the maximum bubble temperature achieved at the complete bubble collapse (T_{max} = 5112 K). The production rate of ·OH radical at the complete bubble collapse at 355 kHz is ~1.5 times lower than that at 515 kHz and ~2.4 times lower than that obtained at the optimum bubble temperature (~4200 K). At 213 kHz, the optimum bubble temperature for the production of ·OH radical is ~4800 K whereas the maximum bubble temperature is 6330 K. In this case, the production rate of ·OH at the complete bubble collapse, which is slightly higher than that at 355 kHz, is ~4 times lower than that obtained at the optimum bubble temperature (~4800 K). As a consequence, the higher sonochemical activity in the case of polyatomic gases, particularly O_2, compared with Ar for frequencies below 515 kHz is not because these gases are dissociated in the bubble and compensate the effect of the lower bubble temperature, but because the oxidants, i.e. ·OH radicals, are strongly consumed inside Ar bubble before the end of the bubble collapse as shown in Fig. 5. The optimum in the production of ·OH results from the competition between the reactions of formation and those of consumption of ·OH at high temperature. The determination of the exact reactions responsible for the consumption and the formation of ·OH is very difficult. However, the most important chemical reactions inside air, O_2 and Ar bubbles have been reported by Yasui and coworkers [34,56] for various bubble temperatures. Nevertheless, on the basis of the results of Fig. 5, it was observed that the competition effect between the reactions of formation and those of consumption is important in the case of Ar than the other gases, which is reflected by an optimum on the curves of Ar at frequencies below 515 kHz.

We will discuss now the effects of the selected gases on the overall sonochemical yield in aqueous solution. Aqueous solution is a multibubble system where a millions of bubbles are expected to be formed [36]. The overall sonochemical activity in aqueous solution depends on the single bubble event as well as the number of bubbles. At fixed operating parameters (frequency, acoustic intensity and liquid temperature), the factor that controls the number of bubbles is the gas solubility. Generally, the higher the gas solubility, the higher will be the nucleation sites for cavitation leading to the higher number of bubbles in the cavitating medium. The solubilities (in mole fraction) of the studied gases are [57]: $x_{Ar} = 2.748 \times 10^{-5}$, $x_{O_2} = 2.517 \times 10^{-5}$, $x_{air} = 1.524 \times 10^{-5}$, $x_{N_2} = 1.276 \times 10^{-5}$. For frequencies above 515 kHz, the gases solubility and the individual chemical bubble yield followed the same order: Ar > O_2 > air > N_2. Thus, there is no doubt that argon achieved the highest overall sonochemical activity when frequency is above 515 kHz (see Table 2) as Ar provided the highest individual chemical bubble yield and the higher number of bubbles. For frequencies below 515 kHz, the overall sonochemical yield (Table 2) follows the order of the individual chemical bubble yield (Fig. 3) rather than that of the solubility. This is attributed to the effect of Argon in this region where the slope of the Ar curve slowdown as observed in Fig. 3.

4. Conclusions

In this work, the effects of argon and polyatomic gases toward sonochemical activity has been numerically studied. Computer calculation of the bubble oscillation and chemical reactions inside a bubble have been performed for various frequencies and saturating gases. The numerical results showed that the production rate of hydroxyl radical (the powerful oxidant created in the bubble) is strongly frequency dependent. The rate of production decreases in the order of Ar > O_2 > air > N_2 for all frequencies above 515 kHz and then Ar losses progressively the first order to the following gases with a gradually decreasing of frequency below 515 kHz up to a final order of O_2 > air ~ N_2 > Ar at 213 kHz. The present study gives a numerical interpretation, which differs from that reported in the literature for the obtained trend. There exists an optimum bubble temperature during collapse at which the chemical bubble yield is higher than that of the maximum bubble temperature achieved in the bubble, phenomenon observed only for an argon bubble at frequencies below 515 kHz. It was concluded that the lower sonochemical activity induced by Ar for frequencies below 515 kHz is mainly due to the forte consumption of radicals inside a bubble prior the complete collapse being reached.

Acknowledgement

The financial support by the Ministry of Higher Education and Scientific Research of Algeria (project No. J0101120120098) is greatly acknowledged.

References

[1] T.G. Leighton, The acoustic bubble, Academic press, London, UK, 1994.
[2] K.S. Suslick, D.J. Flannigan, Inside a collapsing bubble: sonoluminescence and the conditions during cavitation, Annu. Rev. Phys. Chem. 59 (2008) 659–683.
[3] K.S. Suslick, Y. Didenko, M.M. Fang, T. Hyeon, K.J. Kolbeck, W.B. McNamara, M.M. Mdleleni, M.M. Wong, Acoustic cavitation and its chemical consequences, Philos. Trans. R. Soc. A: Math. Phys. Eng. Sci. 357 (1999) 335–353.
[4] Y.G. Adewuyi, Sonochemistry: environmental science and engineering applications, Ind. Eng. Chem. Res. 40 (2001) 4681–4715.
[5] S.J. Putterman, K.R. Weninger, Sonoluminescence: how bubbles turn sound into light, Annu. Rev. Fluid Mech. 32 (2000) 445–476.
[6] M. Capocelli, E. Joyce, A. Lancia, T.J. Mason, D. Musmarra, M. Prisciandaro, Sonochemical degradation of estradiols: incidence of ultrasonic frequency, Chem. Eng. J. 210 (2012) 9–17.
[7] T.J. Mason, A.J. Cobley, J.E. Graves, D. Morgan, New evidence for the inverse dependence of mechanical and chemical effects on the frequency of ultrasound, Ultrason. Sonochem. 18 (2011) 226–230.
[8] P. Kanthale, F. Ashokkumar, F. Grieser, Sonoluminescence, sonochemistry (H_2O_2 yield) and bubble dynamics: frequency and power effects, Ultrason. Sonochem. 15 (2008) 143–150.
[9] R.A. Torres, C. Pétrier, E. Combet, M. Carrier, C. Pulgarin, Ultrasonic cavitation applied to the treatment of bisphenol A. Effect of sonochemical parameters and analysis of BPA by-products, Ultrason. Sonochem. 15 (2008) 605–611.
[10] Y. Jiang, C. Petrier, T.D. Waite, Sonolysis of 4-chlorophenol in aqueous solution: effects of substrate concentration, aqueous temperature and ultrasonic frequency, Ultrason. Sonochem. 13 (2006) 415–422.
[11] M.A. Beckett, I. Hua, Impact of ultrasonic frequency on aqueous sonoluminescence and sonochemistry, J. Phys. Chem. A 105 (2001) 3796–3802.
[12] E.L. Mead, R.G. Sutherland, R.E. Verrall, The effects of ultrasound on water in the presence of dissolved gases, Can. J. Chem. 54 (1976) 1114–1120.
[13] I. Hua, M.R. Hoffmann, Optimization of ultrasonic irradiation as an advanced oxidation technology, Environ. Sci. Technol. 31 (1997) 2237–2243.
[14] D.G. Wayment, D.J. Casadonte, Frequency effect on the sonochemical remediation of alachlor, Ultrason. Sonochem. 9 (2002) 251–257.
[15] F. Guzman-Duque, C. Pétrier, C. Pulgarin, G. Peñuel, R.A. Torres-Palma, Effects of sonochemical parameters and inorganic ions during the sonochemical degradation of crystal violet in water, Ultrason. Sonochem. 18 (2011) 440–446.
[16] Y.-Q. Gao, N.-Y. Gao, Y. Deng, J.-s. Gu, Y.-L. Gu, D. Zhang, Factor affecting sonolytic degradation of sulfamethazine in water, Ultrason. Sonochem. 20 (2013) 1401–1407.
[17] C. Pétrier, A. Jeunet, J.-L. Luche, G. Reverdy, Unexpected frequency effects on the rate of oxidative processes induced by ultrasound, J. Am. Chem. Soc. 114 (1992) 3148–3150.
[18] R. Kidak, N.H. Ince, Effects of operating parameters on sonochemical decomposition of phenol, J. Hazard. Mater. B137 (2006) 1453–1457.
[19] M. Kitajima, S. Hatanaka, S. Hayashi, Mechanism of O_2-accelerated sonolysis of bisphenol A, Ultrasonics 44 (2006) e371–e373.
[20] G. Mark, A. Tauber, R. Laupert, H.-P. Schechmann, D. Schulz, A. Mues, C. Von Sonntag, OH-radical formation by ultrasound in aqueous solution. Part II. Terephthalate and Fricke dosimetry and the influence of various conditions on the sonolytic yield, Ultrason. Sonochem. 5 (1998) 41–52.

[21] S. Merouani, O. Hamdaoui, Y. Rezgui, M. Guemini, Theoretical estimation of the temperature and pressure within collapsing acoustical bubbles, Ultrason. Sonochem. 21 (2014) 53–59.
[22] S. Merouani, O. Hamdaoui, Y. Rezgui, M. Guemini, Sensitivity of free radicals production in acoustically driven bubble to the ultrasonic frequency and nature of dissolved gases, Ultrason. Sonochem. 22 (2015) 41–50.
[23] L.A. Crum, The polytrophic exponent of gas contained within air bubbles pulsating in a liquid, J. Acoust. Soc. Am. 73 (1983) 116–120.
[24] J.B. Keller, I.I. Kolodner, Damping of underwater explosion bubble oscillations, J. Appl. Phys. 27 (1956) 1152–1161.
[25] J.B. Keller, M.J. Miksis, Bubble oscillations of large amplitude, J. Acoust. Soc. Am. 68 (1980) 628–633.
[26] A.J. Colussi, L.K. Weavers, M.R. Hoffmann, Chemical bubble dynamics and quantitative sonochemistry, J. Phys. Chem. A 102 (1998) 6927–6934.
[27] K. Yasui, Effect of non-equilibrium evaporation and condensation on bubble dynamics near the sonoluminescence threshold, Ultrasonics 36 (1998) 575–580.
[28] B.D. Storey, A.J. Szeri, Water vapor, sonoluminescence and sonochemistry, Proc. R. Soc. Lond. A 456 (2000) 1685–1709.
[29] V. Kamath, A. Prosperetti, F.N. Egolfopoulos, A theoretical study of sonoluminescence, J. Acoust. Soc. Am. 94 (1993) 248–260.
[30] S. Fujikawa, T. Akamatsu, Effects of the non-equilibrium condensation of vapour on the pressure wave produced by the collapse of a bubble in a liquid, J. Fluid Mech. 97 (1980) 481–512.
[31] Y. An, Mechanism of single-bubble sonoluminescence, Phys. Rev. E 74 (2006) 026304.
[32] L. Yuan, H.Y. Cheng, M.-C. Chu, P.T. Leung, Physical parameters affecting sonoluminescence: a self-consistent hydrodynamic study, Phys. Rev. E 57 (1998) 4265–4280.
[33] K. Yasui, A new formulation of bubble dynamics for sonoluminescence (PhD thesis), Waseda University, Japan, 1996.
[34] K. Yasui, T. Tuziuti, Y. Iida, H. Mitome, Theoretical study of the ambient-pressure dependence of sonochemical reactions, J. Chem. Phys. 119 (2003) 346–356.
[35] R. Toegel, D. Loshe, Phase diagrams for sonoluminescing bubbles: a comparison between experiment and theory, J. Chem. Phys. 118 (2003) 1863–1875.
[36] S. Merouani, O. Hamdaoui, Y. Rezgui, M. Guemini, A method for predicting the number of active bubbles in sonochemical reactors, Ultrason. Sonochem. 22 (2015) 51–58.
[37] K. Yasui, Effect of surfactants on single-bubble sonoluminescence, Phys. Rev. E 58 (1998) 45604567.
[38] G. Hauke, D. Fuster, C. Dopazo, Dynamic of a single cavitating and reacting bubble, Phys. Rev. E 75 (2007) 066310.
[39] A. Brotchie, F. Grieser, M. Ashokkumar, Effect of power and frequency on bubble-size distributions in acoustic cavitation, Phys. Rev. Lett. 102 (2009) 084302.
[40] S. Merouani, O. Hamdaoui, Y. Rezgui, M. Guemini, Effects of ultrasound frequency and acoustic amplitude on the size of sonochemically active bubbles –theoretical study, Ultrason. Sonochem. 20 (2013) 815–819.
[41] S. Labouret, J. Frohly, Distribution en tailles des bulles d'un champ de cavitation ultrasonore, 10ème Congrès Français d'Acoustique, Lyon, 2010, http://hal.archives-ouvertes.fr/docs/00/55/11/51/PDF/000441.pdf.
[42] K. Yasui, T. Tuziuti, J. Lee, T. Kozuka, A. Towada, The range of ambient radius for an active bubble in sonoluminescence and sonochemical reactions, J. Chem. Phys. 128 (2008) 184705.
[43] J. Lee, M. Ashokkumar, S. Kentish, F. Grieser, Determination of the size distribution of sonoluminescence bubbles in a pulsed acoustic field, J. Am. Chem. Soc. 127 (2005) 16810–16811.
[44] W.-S. Chen, T.J. Matula, L.A. Crum, The disappearance of ultrasound contrast bubbles: observations of bubble dissolution and cavitation nucleation, Ultrasound Med. Biol. 28 (2002) 793–803.
[45] C. Pétrier, M. Micolie, G. Merlin, J.L. Luche, G. Reverdy, Characteristics of pentachlorophenate degradation in aqueous solution by means of ultrasound, Environ. Sci. Technol. 26 (1992) 1639–1642.
[46] R.A. Torres, C. Pétrier, E. Combet, F. Moulet, C. Pulgarin, Bisphenol A mineralization by integrated ultrasound-UV-iron (II) treatment, Environ. Sci. Technol. 41 (2007) 297–302.
[47] K. Yasui, T. Tuziuti, Y. Iida, Optimum bubble temperature for the sonochemical production of oxidants, Ultrasonics 42 (2004) 579–584.
[48] K. Makino, M.M. Mossoba, P. Riesz, Chemical effects of ultrasound on aqueous solutions. Formation of hydroxyl radicals and hydrogen atoms, J. Phys. Chem. 87 (1983) 1369–1377.
[49] S. Merouani, O. Hamdaoui, Y. Rezgui, M. Guemini, Theoretical procedure for the characterization of acoustic cavitation bubbles, Acta Acustica united with Acustica 100 (2014) 823–833.
[50] Y. Nagata, K. Hirai, H. Bandow, Y. Maeda, Decomposition of hydroxybenzoic and humic acids in water by ultrasonic irradiation, Environ. Sci. Technol. 30 (1996) 1133–1138.
[51] E.J. Hart, A. Henglein, Sonochemistry of aqueous solutions: H_2–O_2 combustion in cavitation bubbles, J. Phys. Chem. 91 (1987) 3654–3656.
[52] F. Méndez-Arriaga, R.A. Torres-palma, C. Pétrier, S. Esplugas, Ultrasonic treatment of water contaminated with ibuprofen, Water Res. 42 (2008) 4243–4248.
[53] J. Rooze, E.V. Rebrov, J.C. Schouten, J.T.F. Keurentjes, Dissolved gas and ultrasonic cavitation – a review, Ultrason. Sonochem. 20 (2013) 1–11.
[54] C.F. Beaton, G.F. Hewitt, Physical property data for the design engineer, Hemisphere Publishing Corporation, New York, 1989.
[55] K. Okitsu, T. Suzuki, N. Takenaka, H. Bandow, R. Nishimura, Y. Maeda, Acoustic multibubble cavitation in water: a new aspect of the effect of a rare gas atmosphere on bubble temperature and its relevance to sonochemistry, J. Phys. Chem. B 110 (2006) 20081–20084.
[56] K. Yasui, Effects of volatile solutes on sonoluminescence, J. Chem. Phys. 116 (2002) 2945–2954.
[57] P.G.T. Fogg, W. Gerrard, Solubility of gases in liquids, John Wiley & Sons Ltd., Chichester, UK.